Inorganic Chemistry

Article

pubs.acs.org/IC

Intensive Upconversion Luminescence of Na-Codoped Rare-Earth Oxides with a Novel RE−Na Heterometallic Complex as Precursor

Xiang-Jun Zheng,[†,‡] Ayjamal Ablet,[†] Christie Ng,[‡] and Wing-Tak Wong*[,‡]

[†]Beijing Key Laboratory of Energy Conversion and Storage Materials, College of Chemistry, Beijing Normal University, Beijing, 100875, People's Republic of China

[‡]Department of Applied Biology & Chemical Technology, The Hong Kong Polytechnic University, Hung Hom, Hong Kong SAR, People's Republic of China

Supporting Information

ABSTRACT: Four novel heterometallic RE−Na−organic frameworks, $[(RE)Na_3(PZTC)_2(H_2O)_4]\cdot 2H_2O$ (RE = Yb (**1**), Ho (**2**), Er (**3**), Y (**4**); PZTC = pyrazine-2,3,5-tricarboxylate), were synthesized via solvothermal reactions and characterized by IR, elemental analysis, and single-crystal X-ray diffraction. The results show that the four complexes are isostructural. In the frameworks, the trinuclear Na cluster and RE ion acting as nodes are bridged by the multifunctional PZTC ligand to give a 3-D framework. Codoping in the frameworks was realized due to their isostructural characteristics. The codoped complexes were calcinated at 800 °C to give rise to the corresponding oxides. Investigation of their photophysical properties shows that the upconversion luminescence (UCL) of the Ho system is green while that of the Er system is red upon excitation at 980 nm. With regard to the luminescence color and intensity, the Er system is preferable to the Ho system for application in bioimaging. Both the red and the green UCL of the Ho^{3+} and Er^{3+} systems involve a two-photon process. In addition, the UCL mechanism is given. The UCL comparison of Na-doped oxides with non-Na-doped oxides indicates that doping Na can greatly enhance the UCL of the Er system.

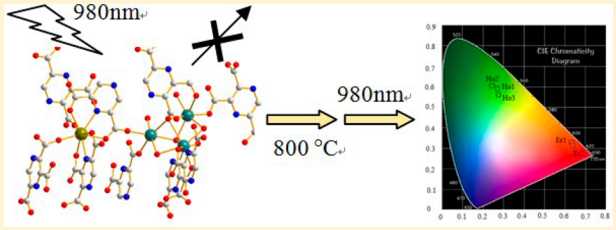

INTRODUCTION

Much effort has been devoted to develop novel fluorescent materials in the fields of biotechnology, photonics, and optoelectronics in the past decade.[1] Lanthanide luminescent materials have aroused growing interest because of their narrow emission band widths (<10 nm), long luminescence lifetime (approximate millisecond range), large anti-Stokes shifts, and high resistance to photobleaching.[2] There are down- and upconversion luminescence processes for lanthanide materials. In the upconversion process, photons with low energy (usually near-infrared photons) are absorbed and photons with high energy are emitted. Lanthanide ions are well-known active ions used to create upconversion luminescence in different host materials. In comparison with quantum dots and organic fluorescent dyes, the upconversion luminescent lanthanide materials are more suitable for various biological applications due to their low toxicity and NIR excitation in the spectral range 700−1000 nm.[3] There are mainly three types of lanthanide upconversion materials: coordination compounds, fluorides, and oxides. Among them, lanthanide coordination compounds are rarely reported[4] because of the strong nonradiative quenching of the lanthanide excitation by the O−H, C−H, and N−H vibrations in the complex.[5] The inorganic fluorides have the advantage of intrinsic low phonon energies (~350 cm^{-1}) and thereby are often employed as host materials.[6] For the inorganic oxide, yttrium oxide (Y_2O_3) as the host for lanthanide ions for optical application[7] has been widely investigated due to its broad transparency range (0.2−8 μm), relatively low phonon cutoff energy, and high thermal stability. For upconversion luminescence, the most commonly used excitation source is a 980 nm laser, which is comparable to the gap between the energy levels of $^2F_{7/2}$ and $^2F_{5/2}$ of the Yb^{3+} ion. Yb^{3+} ion acts as a well-known sensitizer with a large absorption cross-section at ~980 nm for the emission of several lanthanide activators, such as Er^{3+}, Ho^{3+}, and Tm^{3+}. It has been reported that the UCL of the Y_2O_3:Yb^{3+}, Er^{3+} system is 1 or 2 orders of magnitude higher than that without the sensitizer Yb^{3+}.[8] In addition, the incorporation of lithium ions into the Y_2O_3 matrix with Yb^{3+}, Er^{3+} (Ho^{3+} or Tm^{3+}) doped compositions can enhance the upconversion luminescence under 980 nm excitation due to the tailoring effect induced by the Li^+ ions.[9] In the present work, we report a synthetic strategy of Na^+-doped rare-earth oxides, Y_2O_3:Yb^{3+}, Er^{3+} (Ho^{3+}), with a codoped complex as precursor, which enables Na^+ and RE ions present in one complex to provide the possibility of codoping them uniformly in one oxide. Furthermore, we report their UC mechanism, especially the rarely reported intense and pure red emission of the Er^{3+} system.

Received: March 14, 2014
Published: June 13, 2014

   dx.doi.org/10.1021/ic500592k | Inorg. Chem. 2014, 53, 6788−6793

MATERIALS AND METHODS

Pyrazine-2,3,5-tricarboxylic acid (H_3PZTC) dihydrate was synthesized according to the literature.[10] All other chemicals were commercially available and were used as received without further purification. Elemental analyses (CHN) were performed using a Vario EL elemental analyzer. FT-IR spectra were recorded from KBr pellets in the range 4000−400 cm^{-1} on a Nicolet Avatar 360 FT-IR spectrometer. The codoping ratio was confirmed by inductively coupled plasma (ICP) analysis performed with a JY ULTIMA spectrometer. Upconversion luminescence spectra were obtained on a PerkinElmer LS 55 fluorescence spectrophotometer. An external 0−1.3 W adjustable diode laser integrated with an optical fiber (980 nm, Beijing Hi-Tech Optoelectronic Co.,People's Republic of China) was used as the excitation source to replace the original xenon source in the spectrophotometer. Powder X-ray diffraction (PXRD) patterns were recorded on a Rigaku SmartLab X-ray diffractometer for Cu Kα radiation (λ = 1.5406 Å), with a scan speed of 10° min^{-1} and a step size of 0.02° in 2θ.

Synthesis of Complexes 1−4. A mixture of $(RE)Cl_3{\cdot}6H_2O$ (0.1 mmol; RE = Yb (**1**), Ho (**2**), Er (**3**), Y (**4**)), $H_3PZTC{\cdot}2H_2O$ (0.025 g, 0.1 mmol), NaAc−HAc buffer solution (1 mL, pH 5.7), and isopropyl alcohol (1 mL) was sealed in a 23 mL Teflon-lined autoclave and heated under autogenous pressure to 140 °C for 72 h and then cooled to room temperature. Colorless crystals of **1** (0.031 g, 40.4% based on Yb), light yellow crystals of **2** (0.028 g, 36.8% based on Ho), pink crystals of **3** (0.029 g, 38% based on Er), and colorless crystals of **4** (0.030 g, 43.9% based on Y) were obtained by filtration and then dried. Anal. Calcd for $C_{14}H_{14}N_4Na_3O_{18}Yb$: C, 21.89; H, 1.84; N, 7.29. Found: C, 22.21; H, 2.23; N, 7.08. IR (KBr, cm^{-1}): 3418 vs, 1633 vs, 1470 m, 1417 m, 1370 m, 1312 m, 1222 m, 1178 m, 1119 m, 962 w, 845 m, 827 w, 798 w, 756 w, 614 m, 464 w. Anal. Calcd for $C_{14}H_{14}HoN_4Na_3O_{18}$: C, 22.12; H, 1.86; N, 7.37. Found: C, 22.25; H, 2.24; N, 7.40. IR (KBr, cm^{-1}): 3404 vs, 1637 vs, 1473 m, 1395 m, 1369 m, 1312 m, 1222 m, 1182 m, 1119 m, 961 w, 845 m, 826 w, 798 w, 755 w, 613 m, 447 w. Anal. Calcd for $C_{14}H_{14}ErN_4Na_3O_{18}$: C, 22.05; H, 1.85; N, 7.34. Found: C, 22.40; H, 2.19; N, 7.25. IR (KBr, cm^{-1}): 3400 vs, 1637 vs, 1471 m, 1420 m, 1369 m, 1312 m, 1222 m, 1182 m, 1120 m, 962 w, 845 m, 826 w, 798 w, 756 w, 613 m, 468 w. Anal. Calcd for $C_{14}H_{14}N_4Na_3O_{18}Y$: C, 24.58; H, 2.06; N, 8.19. Found: C, 24.86; H, 2.55; N, 8.26. IR (KBr, cm^{-1}): 3419 vs, 1636 vs, 1472 m, 1419 m, 1363 m, 1312 m, 1220 m, 1179 m, 1119 m, 962 w, 845 m, 826 w, 797 w, 754 w, 612 m, 464 w.

Synthesis of Codoped Rare Earth Oxides. *Method 1. Na-Doped Oxides.* The codoped complexes were prepared first by following the synthetic precedure of complex **1** but using $YCl_3{\cdot}6H_2O$, $ErCl_3{\cdot}6H_2O$ ($HoCl_3{\cdot}6H_2O$), and $YbCl_3{\cdot}6H_2O$ in different molar ratios instead of 100% $YbCl_3{\cdot}6H_2O$. The obtained samples of complexes were calcinated at 800 °C for 2 h in an open atmosphere and then cooled to room temperature in the furnace. The obtained white powders were washed with Milli-Q water and centrifuged. The tridoped oxides (Ho1−Ho3, Er1, Er2) were then dried at 105 °C for 3 h to get rid of the solvent. The result of the codoping ratio of rare-earth ions in the sample is shown in Table 1.

Table 1. Codoping Ratio of Yb, Ho(Er), and Y in Different Samples

sample	codoping ratio Yb:Ho(Er):Y
Ho1	10:2:88
Ho2	19:4:77
Ho3	11:5:84
Er1	19:4:77
Er2	10:2:88
Er3	18:2:80
Er4	27:5:68
Er5	60:10:30
Er6	95:5:0

Method 2. Codoped Oxides without Na. A mixture of glycine (0.2 mmol), oxalic acid (0.3 mmol), $(RE)Cl_3$ (0.2 mmol; $YCl_3{\cdot}6H_2O$, $ErCl_3{\cdot}6H_2O$, and $YbCl_3{\cdot}6H_2O$ in different molar ratios), 5 mL of ethanol, and NaOH (0.39 mmol) was sealed in a 23 mL Teflon-lined autoclave and heated under autogenous pressure at 100 °C for 72 h and then cooled to room temperature. The obtained samples of complexes were calcinated at 800 °C for 2 h in an open atmosphere and then cooled to room temperature in the furnace. The obtained bi- and monodoped oxides were named Er3−Er5 and Er6, respectively, as shown in Table 1.

Crystal Structure Determination. Single-crystal X-ray diffraction analyses of the four complexes were carried out on a Bruker APEX II CCD area detector diffractometer equipped with graphite-monochromated Mo Kα radiation (λ = 0.71073 Å). Semiempirical absorption corrections were applied using the SADABS program.[11] The structures were solved by direct methods and refined by full-matrix least squares on F^2 using SHELXS 97 and SHELXL 97 programs.[12,13] All non-hydrogen atoms were refined anisotropically. The hydrogen atoms were set in calculated positions and refined by a riding mode. The crystallographic details of complexes **1**−**4** are provided in Table 2, while selected bond distances and angles are given in Table S1 (Supporting Information).

RESULTS AND DISCUSSION

Synthetic Considerations. To minimize the effect of high vibrations such as C−H and N−H on lanthanide luminescence, a tricarboxylic acid, pyrazine-2,3,5-tricarboxylic acid with only one C−H bond, was synthesized. HAc−NaAc buffer solution (pH 5.7) was utilized to provide Na^+ ion and facilitate the crystallization of heterometallic complexes. The result of single-crystal X-ray diffraction revealed that the Y, Yb, Er, and Ho complexes are isostructural. Then Yb^{3+} was selected as sensitizer and Ho^{3+} and Er^{3+} were used as activators to dope in the Y^{3+} complex. Finally, the resultant codoping complex acted as a precursor to prepare the tridoped oxide with Na^+. For comparison, oxides without Na^+ ion were also prepared with the method of complex as precursor.

Structures of Complexes 1−4. Single-crystal X-ray diffraction studies have revealed that complexes **1**−**4** are isomorphous. Therefore, only the structure of $[YbNa_3(PZTC)_2(H_2O)_4]{\cdot}2H_2O$ (**1**) will be described in detail.

In the asymmetric unit, there is one Yb^{3+} ion, three Na^+ ions, two PZTC ligands, four coordinated water molecules, and two lattice water molecules. The Yb^{3+} ion is eight-coordinated with two nitrogen atoms (N1 and N5A) and six oxygen atoms (O1, O6, O3B, O7, O10A, and O11A) from four PZTC ligands (Figure 1). The Na^+ ions are all six-coordinated with oxygen atoms in an octahedral geometry. Na1 is coordinated with two water molecules (O13 and O16) and four oxygen atoms (O2, O12C, O8E, and O4D) from four PZTC ligands. Na2 is coordinated with two water molecules (O13 and O14) and four oxygen atoms (O7E, O10F, O4D, and O8E) from three PZTC ligands. Na3 is coordinated with two water molecules (O14 and O15) and four oxygen atoms (O5D, O6E, O4D, and O8E) from three PZTC ligands. The Na^+ ions in one asymmetric unit is arrayed in a triangle. Two water molecules (O13 and O14) bridge Na1 and Na2, and Na2 and Na3, respectively, on the triangle plane. Above and below the plane, two carboxylate oxygen atoms (O8 and O4) bridge the three Na^+ ions in a tridentate mode, respectively, forming a trinuclear Na^+ cluster (Figure 1b).

PZTC adopts two types of coordination modes, as shown in Scheme 1. It acts as a bridging ligand in μ_7,η^{10} mode, linking the Yb^{3+} and Na^+ ions to form 3-D coordination polymers with water molecules in the 1-D channels (Figure 2a). The lattice

dx.doi.org/10.1021/ic500592k | Inorg. Chem. 2014, 53, 6788−6793

Table 2. Crystal Data and Structure Refinement Details for Complexes 1−4

	1	2	3	4
empirical formula	$C_{14}H_{14}N_4Na_3O_{18}Yb$	$C_{14}H_{14}HoN_4Na_3O_{18}$	$C_{14}H_{14}ErN_4Na_3O_{18}$	$C_{14}H_{14}N_4Na_3O_{18}Y$
formula wt	768.30	760.19	762.52	684.17
cryst syst	triclinic	triclinic	triclinic	triclinic
space group	$P\bar{1}$	$P\bar{1}$	$P\bar{1}$	$P\bar{1}$
a/Å	8.8112(12)	8.8391(7)	8.8294(9)	8.8392(10)
b/Å	9.2356(12)	9.2446(7)	9.2401(10)	9.2461(10)
c/Å	15.011(2)	15.0589(12)	15.0407(16)	15.0662(16)
α/deg	97.941(2)	98.2180(10)	98.120(2)	98.184(2)
β/deg	106.866(2)	106.5300(10)	106.659(2)	106.541(2)
γ/deg	94.495(2)	94.7320(10)	94.655(2)	94.703(2)
V/Å^3	1148.7(3)	1157.67(16)	1154.2(2)	1158.6(2)
Z	2	2	2	2
D_{calcd}/g cm^{-3}	2.221	2.181	2.194	1.961
μ/mm^{-1}	4.228	3.573	3.792	2.672
no. of collected, unique rflns; R_{int}	5808, 4116; 0.027	6025, 4144; 0.0294	5942, 4126; 0.0374	6063, 4162; 0.0400
R indices (all data)	R1 = 0.0443, wR2 = 0.0716	R1 = 0.0497, wR2 = 0.1217	R1 = 0.0734, wR2 = 0.1377	R1 = 0.0869, wR2 = 0.1283
CCDC no.	980465	980466	980467	980468

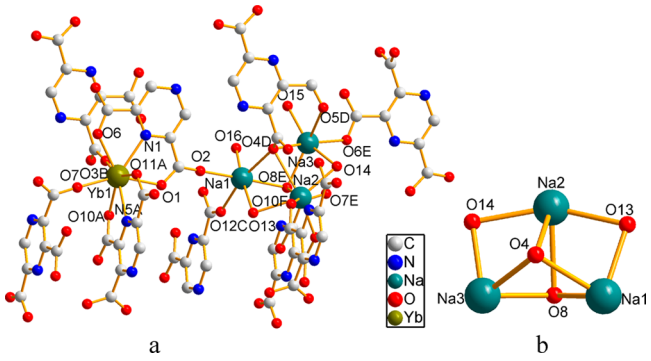

Figure 1. (a) Coordination environment of metal ions in **1**. Symmetry operation: (A) $-x, 2-y, -z$; (B) $1-x, 2-y, 1-z$; (C) $1-x, 2-y, -z$; (D) $1-x, 1-y, 1-z$; (E) $1+x, -1+y, z$; (F) $-x, 1-y, -z$. All hydrogen atoms are omitted for clarity. (b) The trinuclear Na cluster bridged by μ_2-H_2O and μ_3-carboxylate oxygen atom.

Scheme 1. Coordination Mode of PZTC in 1

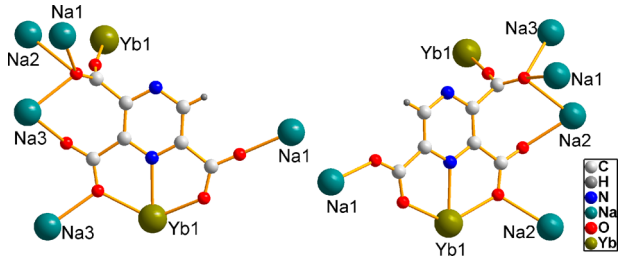

water molecules are located at the channels stabilized via O−H···O or O−H···N hydrogen bonding with the framework (Table S2, Supporting Information).

The total void volume, V_{void}, within complex **1** without water molecules is 14% per unit volume, as determined by PLATON. In order to classify the topology of the network, suitable nodes should be defined. There is one type of Yb^{3+}, two types of PZTC, and three types of Na^+ ions in complex **1** (Scheme 1). The trinuclear Na cluster is considered a six-connected node surrounded by six PZTC ligands. The Yb atom is connected to four PZTC ligands; therefore it is regarded as a 4-connected node. The PZTC ligand connected to two Yb^{3+} ions and three

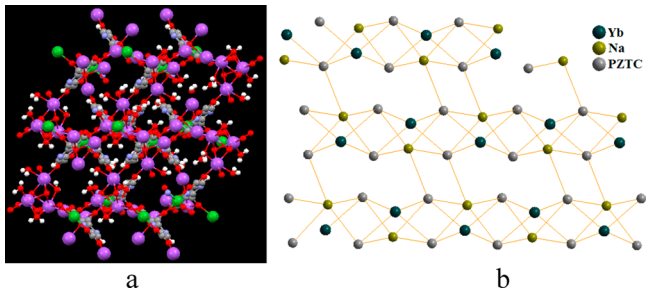

Figure 2. (a) 3-D packing diagram of **1** viewed along the c axis, showing the water molecules in the 1-D channel. (b) 3D topology of complex **1** viewed along the a axis.

Na^+ ions can be considered a 5-connected node. The ligand H_2O is 1- or 2-connected and thus can be omitted when analyzing the topology. Figure 2b shows the topological diagram.

Powder X-ray Diffraction of the Oxides. Figure 3 shows the XRD patterns of the Y_2O_3 powders prepared by calcinating the complexes doped with Er(Ho) and Yb ions in different ratios using two methods. All powders have a cubic structure (space group $Ia3$) corresponding to the standard pattern of Y_2O_3 (JCPDS 41-1105). No impurity peak is observed in the pattern, which confirms the phase purity of the samples. ICP results show that the codoping ratio of Na^+ ion in the tridoped sery is about 23%.

Upconversion Luminescence of Codoped RE Oxides. Although there is no water molecule coordinated to the RE ion, there are four coordinating water molecules for Na^+ ions and two lattice water molecules per asymmetric unit for RE−Na complexes. It is known that the O−H oscillator is apt to quench the luminescence of RE ions.[5] Therefore, there is no upconversion luminescence observed for the series of codoped complexes excited at 980 nm with a power of up to 1.064 W. However, when the samples were calcinated to prepare the corresponding oxides, strong green and red emissions could be seen with the naked eye for the Ho- and Er-doped samples, respectively. For the Ho-doped oxide, upon excitation at 980 nm, there is an intense emission at 544 nm and a weak emission at 657 nm (Figure 4a), which can be ascribed to the $^5S_2 \rightarrow {}^5I_8$ and $^5F_5 \rightarrow {}^5I_8$ transitions, respectively. Furthermore, the colors

dx.doi.org/10.1021/ic500592k | Inorg. Chem. 2014, 53, 6788−6793

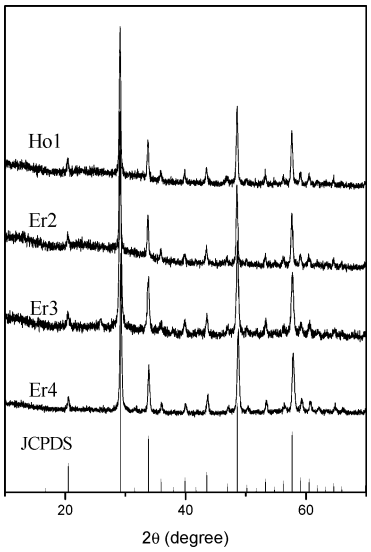

Figure 3. Powder X-ray diffraction patterns of samples of Ho1, Er2–Er4, and the standard pattern of JCPDS 41-1105.

of samples Ho1–Ho3, Er1, and Er2 in terms of mathematically defined color space were studied. The CIE chromaticity diagram (Figure 5) indicates that the Ho systems (Ho1–Ho3) are green with CIE chromaticity coordinates of (0.2692 0.5644), (0.2509 0.6135), and (0.2671 0.5950), respectively, upon excitation at 980 nm. For the Er-doped oxide (Er1, Er2), there is an intense emission at 659 nm corresponding to the $^4F_{9/2} \rightarrow {}^4I_{15/2}$ transition and a very weak emission at 548 nm (Figure 4b) corresponding to the $^4S_{3/2} \rightarrow {}^4I_{15/2}$ transition. For the Er2 sample, the red emission in the range 620–720 nm is about 13.5 times the green emission in the range 500–600 nm. The CIE chromaticity diagram indicates that the Er systems (Er1, Er2) are red with CIE chromaticity coordinates of (0.6236 0.3391) and (0.6305 0.3298), respectively, upon excitation at 980 nm. Coordinates located at the boundary (Figure 5) indicate the high color purity of samples. Figure 4b shows that the Er system (Er2) with the codoping ratio Y:Er:Yb = 88:2:10 displays an upconversion luminescence (more intense more than 1.5 times) than that of Er1 (77:4:19). A comparison between the Ho system and the Er system with the same codoping ratio (Figure 4c) shows that the green emission of the Ho system is slightly stronger than that of the Er system but the red emission of the Er system is about 17 times greater than that of the Ho system, even with a smaller slit. This may be attributed to the matching of the resonant energy level of Er^{3+} with Yb^{3+}, which is beneficial to the energy transfer from Yb^{3+} to Er^{3+} ion. As is known, red emission has more advantages than green emission in bioimaging because it can penetrate biotissues more deeply owing to its longer wavelength.[14] To our knowledge, there are few reports about the red UC emission of Er^{3+}-doped Y_2O_3. Therefore, for the title codoped oxides, Er is preferable to Ho as an activator to obtain upconversion luminescence for bioimaging.

As is known, the log value of UC emission intensity is proportional to the log value of applied laser input power. The slope of the curve (log I versus log P) gives out the number of photons involved in the excitation process of different emission bands. Therefore, a laser input power dependence study was carried out. The results (insets in Figure 4a,b) show that both the red and green emissions of the Ho system and Er system involve a two-photon process. Figure 6 shows the upconversion

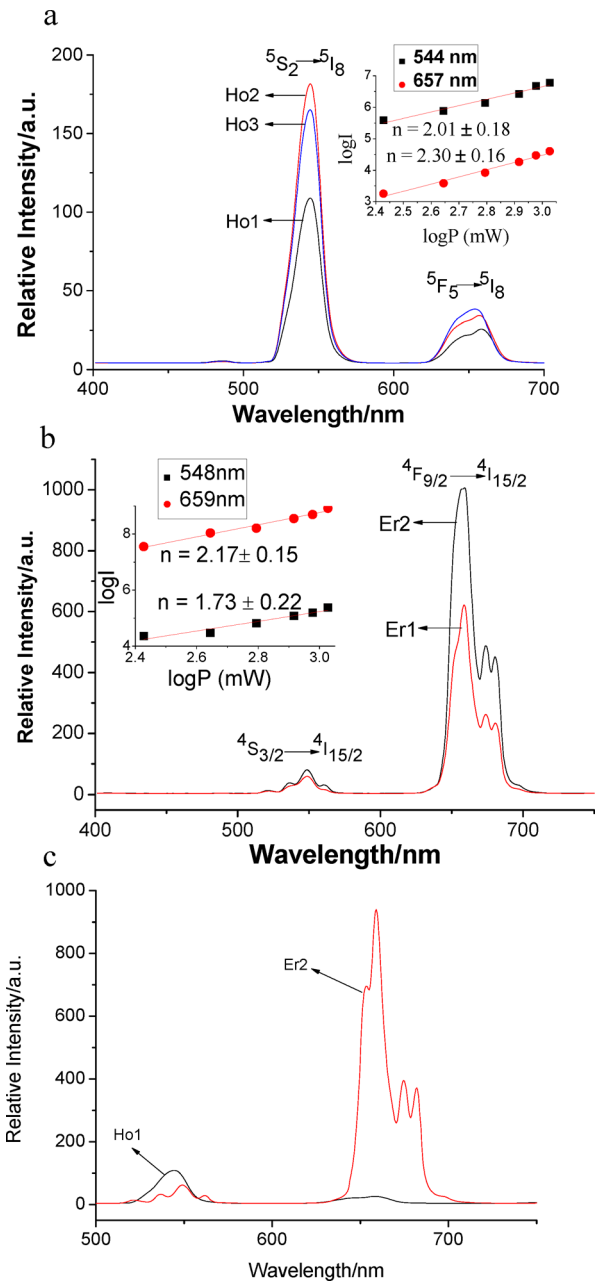

Figure 4. Upconversion luminescence spectra of different samples excited at 980 nm: (a) Ho1–Ho3, slit 15 nm, P = 1.064 W; (b) Er1–Er2, slit 7 nm, P = 0.623 W; (c) comparison between the Er and Ho systems with the same codoping ratio and experimental conditions except slit 5.5 nm for Er2 and slit 15 nm for Ho1, P = 1.064 W.

mechanism of the green and red emissions of Ho and Er systems. As shown in Figure 6, for the Er system, the Yb^{3+} ion was first excited by a 976 nm photon from the $^2F_{7/2}$ level to the excited $^2F_{5/2}$ state. The energy was then transferred from Yb^{3+} to Er^{3+} to promote the Er^{3+} ion from the $^4I_{15/2}$ state to the $^4I_{11/2}$ state. Then a second photon was absorbed to pump Er^{3+} ion to the $^4F_{7/2}$ state. The nonradiative relaxation makes the $^4S_{3/2}$ state populated. The Er^{3+} ion in the $^4S_{3/2}$ states emits in the green range (548 nm) on going back to the ground state $^4I_{15/2}$. For the red emission at 659 nm generated by the $^4F_{9/2}$ to $^4I_{15/2}$ transition, there are two possible routes. First, the state $^4F_{9/2}$ can be reached by the nonradiative decay from the $^4S_{3/2}$ state. In the second possible route, Er^{3+} ion in the $^4I_{11/2}$ state loses its

dx.doi.org/10.1021/ic500592k | Inorg. Chem. 2014, 53, 6788–6793

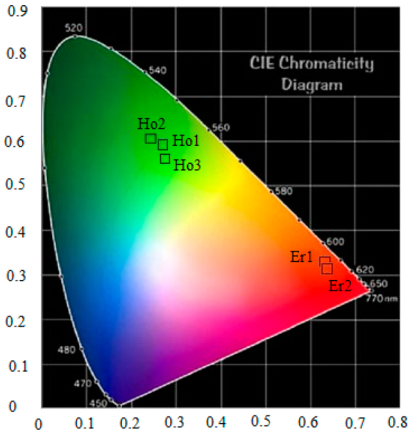

Figure 5. CIE chromaticity diagram of oxides Ho1–Ho3, Er1, and Er2.

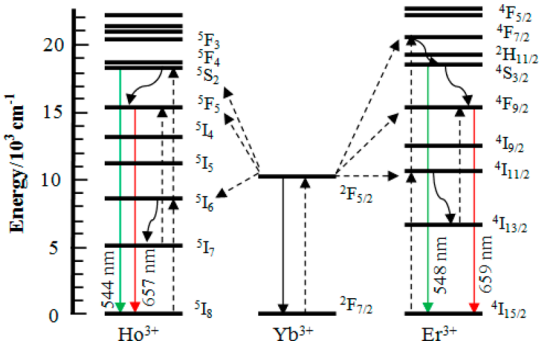

Figure 6. Energy level diagrams of the Ho^{3+}, Er^{3+}, and Yb^{3+} ions as well as the proposed UC mechanisms for the green and red emissions.

energy in going to the $^4I_{13/2}$ level with some nonradiative decay involved. Then a second photon pumps the Er^{3+} from the $^4I_{13/2}$ state to the $^4F_{9/2}$ level, and thus the red emission is obtained. For the Ho system, the green emission (544 nm) and red emission (657 nm) are generated from the transitions of $^5S_2$ and $^5F_5$ to the ground state $^5I_8$, respectively. There are also two possible routes for the red emission, as shown in Figure 6.

For comparison, the bidoped oxides Y_2O_3:Yb, Er and monodoped oxide Yb_2O_3:Er without Na^+ ion were prepared by method 2. Their upconversion luminescence spectra are shown in Figure 7. It can be seen that the luminescence

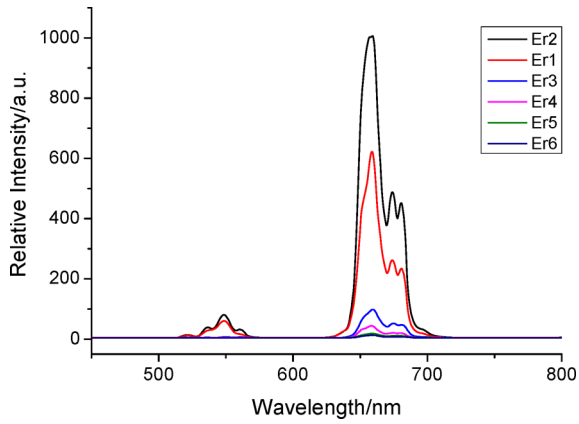

Figure 7. Emission of mono-, bi-, and tridoped Er systems with and without Na^+ ion (slit 7 nm, P = 0.623 W, λ_{ex} 980 nm).

intensity decreases in the order Er3 > Er4 > Er5 > Er6. This may be attributed to the decreasing molar ratio of matrix Y, which leads to the increasing amount of Yb^{3+} and Er^{3+} and consequently the interion quenching of the luminescence. Under the same conditions, the upconversion luminescence of the bidoped Er system without codoped Na (Er3–Er6) is much weaker than those tridoped with Na (Er1, Er2). In addition, even the luminescence of the monodoped system (Er6) is low. As is known, the doping of Li^+ ion can change the local crystal field around the lanthanide activator ions to intermix the f states of lanthanides with higher electronic configurations, thus making the transition probability flexible.[15] For the C-type cubic bixbyite Y_2O_3, the cations are all six-coordinated. As shown in Table S3 (Supporting Information), the ionic size of Na^+ is larger than that of the rare-earth ions Yb^{3+}, Er^{3+}, Y^{3+}, and Ho^{3+}. Therefore, Na^+ may substitute the site of the rare-earth ion instead of the interstitial occupation.[15b] It can be concluded that doping Na^+ ion can also make the transition probability flexible. As a consequence, the UC luminescence was enhanced dramatically. In other words, the tridoped system Y_2O_3:Yb, Er, Na is efficient for obtaining upconversion luminescence excited by a near-infrared laser at 980 nm, and our strategy to dope Na^+ in the tridoped oxide system based on the RE-Na heterometallic complex is effective.

CONCLUSION

Four new metal–organic frameworks were synthesized via solvothermal conditions. Na-containing tridoped oxides were obtained by calcinating the codoped RE–Na heterometallic complexes. We verified that the strategy to increase the upconversion luminescence of Yb- and Er-doped Y_2O_3 on the basis of the codoping of Na^+ ion was effective. For the tridoped oxide system, the Er system is preferable to the Ho system when emission intensity and application for bioimaging are taken into consideration. Moreover, Y_2O_3:Yb, Er, Na materials have the potential to be used in living cell bioimaging.

ASSOCIATED CONTENT

Supporting Information

Tables, figures, and CIF files giving X-ray crystallographic data and selected bond angles and distances for complexes **1**–**4**, the hydrogen-bonding geometry in complex **1**, and ionic sizes of elements. This material is available free of charge via the Internet at http://pubs.acs.org.

AUTHOR INFORMATION

Corresponding Author

*E-mail for W.-T.W.: wing-tak.wong@polyu.edu.hk.

Notes

The authors declare no competing financial interest.

ACKNOWLEDGMENTS

This work was supported by the National Natural Science Foundation of China (20971015), the Hong Kong Scholar Program, the Fundamental Research Funds for the Central Universities, and the Hong Kong Research Grants Council.

REFERENCES

(1) (a) Burns, A.; Ow, H.; Weisner, U. *Chem. Soc. Rev.* **2006**, *35*, 1028–1042. (b) Das, G. K.; Tan, T. T. Y. *J. Phys. Chem. C* **2008**, *112*, 11211–11217. (c) Coe, S.; Woo, W. K.; Bawendi, M.; Bulovic, V. *Nature* **2002**, *420*, 800–803.

(2) Mishra, K.; Singh, S. K.; Singh, A. K.; Rai, S. B. *Mater. Res. Bull.* **2013**, *48*, 4307−4313.
(3) (a) Nichkova, M.; Dosev, D.; Gee, S. J.; Hammock, B. D.; Kennedy, I. M. *Anal. Chem.* **2005**, *77*, 6864−6873. (b) Goldys, E. M.; Tomsia, K. D.; Jinjun, S.; Dosev, D.; Kennedy, I. M.; Yatsunenko, S.; Godlewski, M. *J. Am. Chem. Soc.* **2006**, *128*, 14498−14505. (c) Gordon, W. O.; Carter, J. A.; Tissue, B. M. *J. Lumin.* **2004**, *108*, 339−342.
(4) (a) Hernandez, I.; Pathumakanthar, N.; Wyatt, P. B. *Adv. Mater.* **2010**, *22*, 5356−5360. (b) Weng, D. F.; Zheng, X. J.; Jin, L. P. *Eur. J. Inorg. Chem.* **2006**, 4184−4190. (c) Sun, C. Y.; Zheng, X. J.; Chen, X. B.; Li, L. C.; Jin, L. P. *Inorg. Chim. Acta* **2009**, *362*, 325−330. (d) Weng, D. F.; Zheng, X. J.; Chen, X. B.; Li, L. C.; Jin, L. P. *Eur. J. Inorg. Chem.* **2007**, *21*, 3410−3415.
(5) Tan, R. H. C.; Motevalli, M.; Abrahams, I.; Wyatt, P. B.; Gillin, W. P. *J. Phys. Chem. B* **2006**, *110*, 24476−24479.
(6) (a) Liu, Q.; Feng, W.; Yang, T. S.; Yi, T.; Li, F. Y. *Nat. Protoc.* **2013**, *8*, 2033−2044. (b) Wang, F.; Han, Y.; Lim, C. S.; Lu, Y. H.; Wang, J.; Xu, J.; Chen, H. Y.; Zhang, C.; Hong, M. H.; Liu, X. G. *Nature* **2010**, *463*, 1061−1065. (c) Zeng, S. J.; Tsang, M. K.; Chan, C. F.; Wong, K. L.; Hao, J. H. *Biomaterials* **2012**, *33*, 9232−9238. (d) Jin, J. F.; Gu, Y. J.; Man, C. W.Y.; Cheng, J. P.; Xu, Z. H.; Zhang, Y.; Wang, H. S.; Lee, V. H. Y; Cheng, S. H.; Wong, W. T. *ACS Nano* **2011**, *5*, 7838−7847. (e) Chen, Z. G.; Chen, H. L.; Hu, H.; Yu, M. X.; Li, F. Y.; Zhang, Q.; Zhou, Z. G.; Yi, T.; Huang, C. H. *J. Am. Chem. Soc.* **2008**, *130*, 3023−3029. (f) Liu, Q.; Sun, Y.; Yang, T. S.; Feng, W.; Li, C. G.; Li, F. Y. *J. Am. Chem. Soc.* **2011**, *133*, 17122−17125. (g) Liu, Y.; Chen, M.; Cao, T. Y.; Sun, Y.; Li, C. Y.; Liu, Q.; Yang, T. S.; Yao, L. M.; Feng, W.; Li, F. Y. *J. Am. Chem. Soc.* **2013**, *135*, 9869−9876.
(7) (a) Vetrone, F.; Boyer, J. C.; Capobianco, J. A.; Speghini, A.; Bettinelli, M. *J. Phys. Chem. B* **2003**, *107*, 1107−1112. (b) Wang, H.; Uehara, M.; Nakamura, H.; Miyazaki, M.; Maeda, H. *Adv. Mater.* **2005**, *17*, 2506−2509. (c) Camenzind, A.; Strobel, R.; Pratsinis, S. E. *Chem. Phys. Lett.* **2005**, *415*, 193−197. (d) Muenchausen, R. E.; Jacobsohn, L. G.; Bennett, B. L.; McKigney, E. A.; Smith, J. F.; Valdez, J. A.; Cooke, D. W. *J. Lumin.* **2007**, *126*, 838−842.
(8) Bai, X.; Song, H. W.; Pan, G. H.; Lei, Y. Q.; Wang, T.; Ren, X. G.; Lu, S. Z.; Dong, B.; Dai, Q. L.; Fan, L. B. *J. Phys. Chem. C* **2007**, *111*, 13611−13617.
(9) (a) Stanton, I. N.; Ayres, J. A.; Therien, M. J. *Dalton Trans.* **2012**, *41*, 11576−11578. (b) Chen, G. Y.; Liu, H. C.; Liang, H. J.; Somesfalean, G.; Zhang, Z. G. *J. Phys. Chem. C* **2008**, *112*, 12030−12036. (c) Bai, Y. F.; Wang, Y. X.; Peng, G. Y.; Yang, K.; Zhang, X. R.; Song, Y. L. *J. Alloys Compd.* **2009**, *478*, 676−678.
(10) (a) Mager, H. I. X.; Berends, W. *Recl. Trav. Chim. Pays-Bas* **1958**, *77*, 827−841. (b) Weygand, F. *Chem. Ber.* **1940**, *73*, 1259−1278. (c) Weygand, F.; Bergmann, C. *Chem. Ber.* **1947**, *80*, 255−261.
(11) Sheldrick, G. M. *SADABS, Program for Empirical Absorption Correction of Area Detector Data*; University of Göttingen, Göttingen, Germany, 1997.
(12) Sheldrick, G. M. *SHELXS 97, Program for Crystal Structure Solution*, University of Göttingen, Göttingen, Germany, 1997.
(13) Sheldrick, G. M. *SHELXL 97, Program for Crystal Structure Refinement*, University of Göttingen, Göttingen, Germany, 1997.
(14) (a) Yin, W. Y.; Esposito, D. V.; Yang, S. Z.; Ni, C. Y.; Chen, J. G.; Zhao, G. L.; Zhang, Z. J.; Hu, C. W.; Cao, M. H.; Wei, B. Q. *J. Phys. Chem. C* **2010**, *114*, 13234−13240. (b) Niu, W. B.; Wu, S. L.; Zhang, S. F. *J. Mater. Chem.* **2010**, *20*, 9113−9117. (c) Yi, G. S.; Peng, Y. F.; Gao, Z. Q. *Chem. Mater.* **2011**, *23*, 2729−2734. (d) Yin, W. Y.; Zhao, L. N.; Zhou, L. J.; Gu, Z. J.; Liu, X. X.; Tian, G.; Jin, S.; Yan, L.; Ren, W. L.; Xing, G. M.; Zhao, Y. L. *Chem. Eur. J.* **2012**, *18*, 9239−9245.
(15) (a) Auzel, F. *Chem. Rev.* **2004**, *104*, 139−173. (b) Dou, Q. Q.; Zhang, Y. *Langmuir* **2011**, *27*, 13236−13241.